

https://doi.org/10.1070/QEL16542

Optical properties of heavily ytterbium- and fluorine-doped aluminosilicate core fibres

M.V. Yashkov, A.N. Abramov, A.N. Gur'yanov, M.A. Melkumov, A.V. Shubin, M.M. Bubnov, M.E. Likhachev

Abstract. **An improved MCVD process has been proposed which allows one to fabricate ytterbium-doped fibre preforms with a fluorine-doped aluminosilicate glass-based core. Using this process, we have demonstrated the possibility of codoping the glass with high Yb^{3+} concentration (about 2 wt%), high fluorine concentration (2 wt%) and aluminium oxide concentration above 1.5 mol% (to ensure high ytterbium solubility), resulting in a record low refractive index of the glass ($\Delta n \approx 0.000-0.003$). A series of fibre with a $SiO_2-Al_2O_3-GeO_2-Yb_2O_3-F$ core have been fabricated and their optical characteristics have been investigated. In particular, we have demonstrated the possibility of reaching the highest possible lasing efficiency (82.7% with respect to absorbed pump power). We have studied the photodarkening level in the fibres as a function of ytterbium concentration and demonstrated the feasibility of making ytterbium-doped fibre amplifiers based on the described fibres, with an extremely low output power degradation rate (less than 20% after 10 000 h of continuous operation).**

Keywords: *ytterbium-doped optical fibre, fibre laser, photodarkening, large mode field diameter fibres.*

1. Introduction

At present, rare-earth-doped optical fibres with an increased fundamental mode field diameter are widely used in producing high average and peak power fibre lasers and amplifiers. The key requirements for such fibres are single- or few-mode operation, an increased core diameter (and, as a consequence, an increased mode field diameter) and high rare-earth concentration (to reduce the working fibre length). It is worth noting that the last two requirements, necessary for reducing the influence of nonlinear effects, are mutually exclusive. The point is that, to improve rare-earth solubility at high doping levels, the core glass should be additionally doped with a rather high Al_2O_3 or P_2O_5 concentration [1]. Like the rare-earth oxides, both additives considerably increase the refractive index of silica glass ($\Delta n \approx 0.01$). As a result, to ensure single-mode operation of the active fibre, it is necessary to reduce the fibre core diameter (and, accordingly, the mode area). This leads to a considerable decrease in the threshold for undesirable nonlinear effects.

The refractive index of a fibre core doped with high concentrations of rare-earth ions can be reduced using two approaches. One of them is codoping with aluminium and phosphorus oxides, which reduces the refractive index of the glass almost to the level of silica glass, whereas rare-earth solubility remains sufficiently high [2]. Using this approach, we were able to produce an ytterbium-doped (2 wt%) fibre with a refractive index of its core at a level of 0.0025 and high resistance to photodarkening [3]. However, in the case of an aluminophosphosilicate host, the refractive index of the core cannot be further reduced without reducing the percentage of ytterbium oxide, which produces considerable refractivity (variously reported to be from 0.0008 to 0.0012 per weight percent [4, 5]).

The other approach is additional doping of an aluminosilicate glass host with fluorine, which considerably reduces the refractive index of the glass. In spite of the higher sensitivity of aluminosilicate glass to photodarkening, the latter approach appears rather promising. First, the highest fluorine doping level obtained to date in silica glass in the MCVD process enables a considerable decrease in refractive index ($\Delta n = -0.012$) [6], which, in theory, allows one to compensate for the increase in refractive index in response to doping with high aluminium oxide and rare earth concentrations. Second, the absorption cross section of ytterbium ions may vary by a factor of 2 depending on the glass host, with the highest level offered by aluminosilicate glass-based fibres [7]. This leads to a larger pump absorption coefficient at a given ytterbium concentration and, hence, to a smaller optimal fibre length in lasers and a higher threshold for nonlinear effects.

Despite the promise offered by heavily fluorine doped aluminosilicate hosts, use is currently made of ytterbium-doped active aluminosilicate fibres with a relatively low fluorine content, no higher than 1 wt% [8–11] (corresponding, according to different reports, to a refractive index depression $\Delta n = -0.004 \pm 0.0004$ [8, 12, 13]), which is due to technical problems in the preparation of glass with this composition.

In this paper, we report the preparation and properties of fibres with a $SiO_2-Al_2O_3-(GeO_2)-Yb_2O_3$ glass core additionally doped with ~ 2 wt% fluorine. We have prepared test fibres with a record-breaking cladding pump absorption and studied their basic properties, such as lasing and amplification efficiency and resistance to photodarkening.

2. Fabrication of test preforms and fibres

Fibre preforms were produced by the modified chemical vapour deposition (MCVD) process [14]. The precursors used

M.V. Yashkov, A.N. Abramov, A.N. Gur'yanov G.G. Devyatykh Institute of Chemistry of High-Purity Substances, Russian Academy of Sciences, ul. Tropinina 49, 603950 Nizhnii Novgorod, Russia; **M.A. Melkumov, A.V. Shubin, M.M. Bubnov, M.E. Likhachev** Fiber Optics Research Center, Russian Academy of Sciences, ul. Vavilova 38, 119333 Moscow, Russia; e-mail: likhachev@fo.gpi.ru

Received 20 October 2017
Kvantovaya Elektronika **47** (12) 1099–1104 (2017)
Translated by O.M. Tsarev

in the preparation of the core glass were high-purity $SiCl_4$, $GeCl_4$, $AlCl_3$ and $Yb(tdh)_3$. The MCVD apparatus was supplemented with a system for the evaporation of $AlCl_3$ and volatile rare-earth complexes at temperatures in the range $\sim 130-200\,^{\circ}C$ and vapour delivery. As substrate tubes, we used Heraeus Suprasil F-300 silica tubes. SiF_4 was used as an optimal fluorinating agent because, unlike in the case of other precursors (CF_2Cl_2, $C_2F_3Cl_3$, C_6F_{14} or SF_6), this ruled out an intermediate SiF_4 formation step, which otherwise might have led to SiO_2 losses (as a result of etching) and complicated control over Δn in the preform. In the preform fabrication process, all of the vapour mixture components were simultaneously delivered through heated lines to the reaction zone, where they formed oxide particles, which were then sintered by a burner to give a transparent glass layer. The core diameter was determined by the amounts of the precursors consumed and the number of glass layers produced.

According to our results, glass is difficult to codope with fluorine, aluminium and ytterbium because the addition of SiF_4 to a vapour mixture leads to the formation of the highly volatile compounds AlF_3 and YbF_3, which degrade the efficiency and uniformity of the deposition of the glass components along the length of the preform. These compounds were formed not only in the reaction zone of the major vapour mixture components but also upstream of the reaction zone, at lower temperatures. This led to their premature condensation on the wall of the substrate tube as it cooled. As a consequence, the aluminium oxide concentration along the length of the preform became nonuniform, which in turn led to variations in the refractive index. By additionally heating that part of the substrate tube where uncontrolled AlF_3 and/or YbF_3 condensation took place and adjusting the composition and flow rates of the reactants, we were able to obtain preforms with sufficiently uniform longitudinal dopant profiles.

At present, essentially all high-power fibre lasers are cladding-pumped [10, 11, 15]. The proposed process for the preparation of $SiO_2-Al_2O_3-GeO_2-Yb_2O_3-F$ glasses with a refractive index approaching that of silica glass allows us to fabricate optical fibres with a partially Yb-doped reflective cladding having the same refractive index as undoped silica glass. Fibres of this design have an increased absorption coefficient for pump light propagating in the cladding. Figure 1 shows the refractive index profile and elemental composition of such a preform. It is seen that the glass layer at radii in the range 0.95–1.15 mm is an Yb-doped reflective cladding. According to our estimates, such a layer causes a negligible increase in cutoff wavelength, but increases cladding pump absorption by at least 50%.

This preform was used to produce fibre with a multielement first cladding [15] (Fig. 2a), in which the diameters of the active and passive cores were 90 and 115 μm, respectively. The diameters of both the active and passive fibres were chosen near the minimum possible ones in order to maximise the cladding pump absorption (absorption increases with decreasing undoped silica glass area). Standard fibre cleavers and fusion splicers can be used at silica fibre diameters no less than 80 μm. In our case, the active fibre diameter was 90 μm. The core diameter in the output fibre pigtails of pump diodes is 105–110 μm, so to minimise the fusion splice loss the diameter of the passive fibre (used for pump incoupling) was chosen to be 115 μm.

To ensure anisotropy in the core region and make the fibre polarisation-maintaining, the active fibre had borosilicate glass insets throughout its length. Figure 2b shows the refractive index profiles of the active fibre in the plane passing through the borosilicate rods and in a perpendicular plane. The cladding pump absorption at a wavelength of 915 nm exceeds 3 dB m^{-1} (Fig. 2c), which is at least a factor of 1.5 higher than that in commercially available fibres (single-core fibres with core and cladding diameters of 10–12 and 125 μm [see e.g. Nufern fibres: www.nufern.com)]. In the multielement-cladding fibres, the volume of the silica glass slightly exceeds that in single-element-cladding fibres, which is due to the presence of an additional silica fibre for launching the pump power. Under identical conditions (if the existing commercially available fibres had the same configuration as the multielement-cladding fibre), the gain would be even higher: the cladding pump absorption would then be twice that in its analogues.

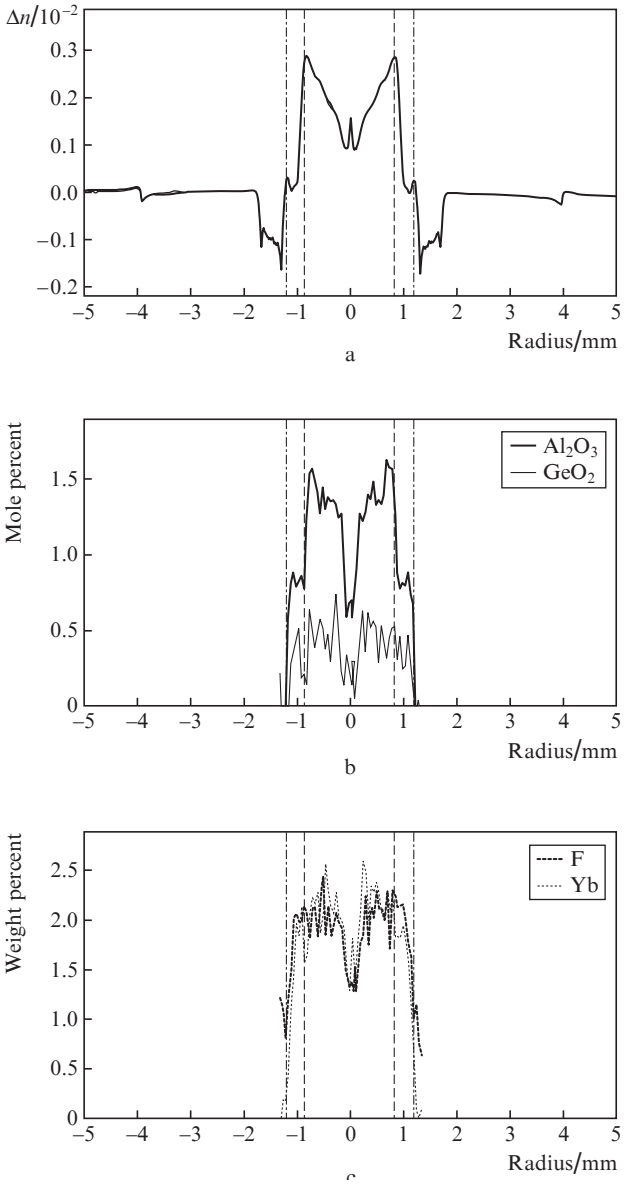

Figure 1. (a) Refractive index profile of preform Y408 (measured with a York Technology P102 preform analyser) and (b, c) elemental composition of the preform core (determined on a JEOL JSM-5910 LV scanning electron microscope, Shared Analytical Facilities Center, Fiber Optics Research Center, Russian Academy of Sciences).

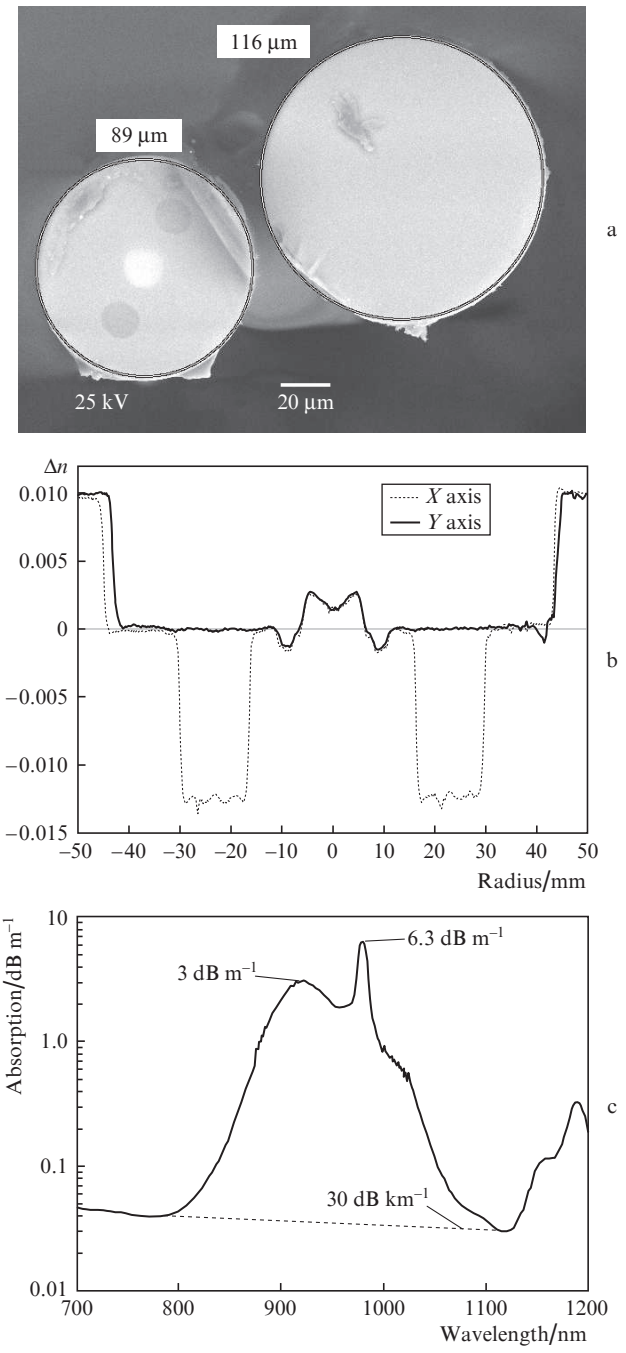

Figure 2. (a) Cross-sectional electron micrograph of the silica fibres in the multielement cladding fibre; (b) refractive index profiles of the fibre which were measured with an EXPO NR200HR analyser along the *X* axis (passing through the borosilicate rods) and the *Y* axis (perpendicular to the plane of the rods); (c) first cladding pump absorption spectrum.

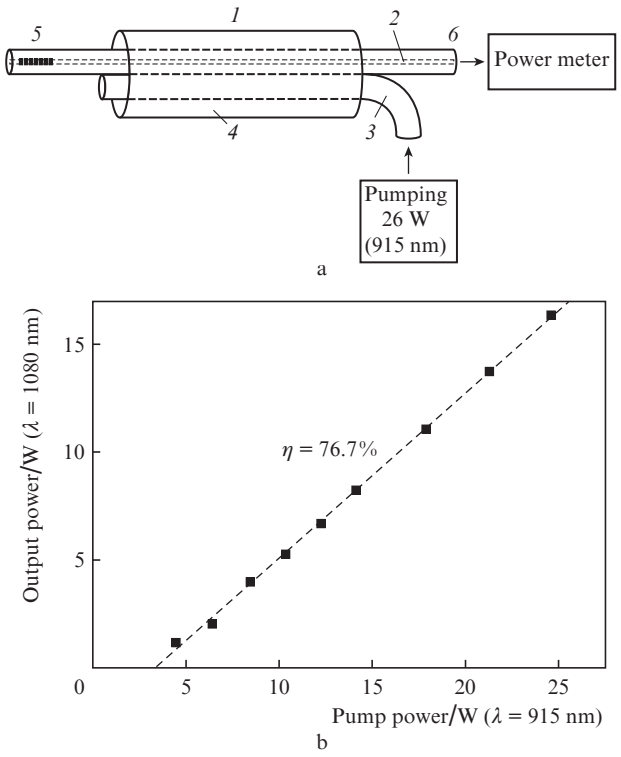

Figure 3. Laser based on the multielement-cladding fibre;
(a) schematic of the laser:
(*1*) test fibre with a multielement first cladding 6.2 m in length; (*2*) ytterbium-doped core fibre drawn out from preform Y408; (*3*) silica fibre for pump incoupling; (*4*) common reflective polymer cladding with an aperture NA > 0.4; (*5*) in-fibre Bragg grating (R = 99%); (*6*) 4% reflecting perpendicular cleave of the fibre end face;
(b) pump-to-laser signal power conversion efficiency.

3. Optical characteristics of the fibres

We measured the pump-to-signal power conversion efficiency in the fibre under study using a counterpropagating pump configuration (Fig. 3a). A fibre Bragg grating (FBG) with a centre wavelength of 1080 nm was written into a separate Flex 1060 fibre and fusion-spliced to the active fibre of the multielement-cladding fibre. For pumping, we used an ~915-nm PUMA fibre-pigtailed diode module (MILON Group) with an output power of up to 26 W. The laser slope efficiency was determined to be 76.7% with respect to launched pump power (Fig. 3b) and 82.7% with respect to absorbed pump power. This efficiency approaches the highest possible quantum efficiency of 915-nm pump conversion to a 1080-nm signal: 84.7%. This confirms the high quality of the fibre and demonstrates that the configuration chosen, in which a considerable fraction of active Yb ions are in effect outside the core (outside the region where Δn exceeds that in the cladding), works well. This approach is only possible owing to the addition of high fluorine concentration to the fibre region doped with Yb and Al.

Figure 4 shows a schematic of an amplifier and the measured efficiency of pump conversion to a signal generated by a single-mode ytterbium fibre laser (λ = 1064 nm) with a power of up to 200 mW. In this case, the differential pump-to-signal power conversion efficiency is about 63%, which is also a good value.

One key characteristic of ytterbium-doped fibres is the rate of photodarkening (a gradual increase in the optical loss in fibres during continuous operation in a laser or amplifier [16]). In fibre sources, the photodarkening of active fibres shows up as a gradual reduction in output power in the course of their operation. After pumping is ceased, the properties of the active fibre may be only partially restored. The photodarkening rate determines the rate of the increase in photoinduced losses in the fibre and, hence, the time the fibre will be able to operate in a device. The loss saturation level and the rate of the increase in photoinduced losses in Yb-doped fibres depend on population inversion and fibre composition. The

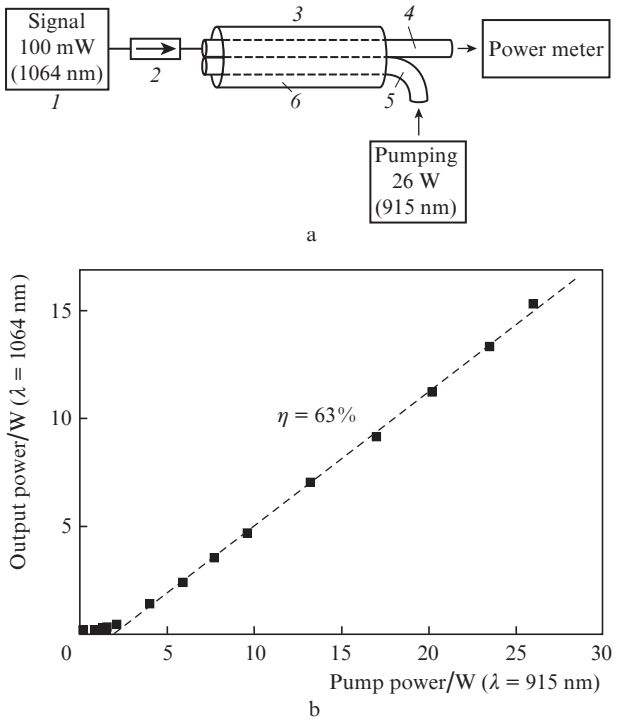

Figure 4. Counterpropagating laser signal amplifier based on the multielement cladding fibre;
(a) schematic of the amplifier:
(*1*) cw Yb-doped fibre laser (100 mW, 1064 nm); (*2*) isolator; (*3*) test fibre with a multielement first cladding; (*4*) ytterbium-doped core fibre drawn out from preform Y408; (*5*) silica fibre for pump incoupling; (*6*) common reflective polymer cladding with an aperture NA > 0.4;
(b) measured pump-to-laser signal power conversion efficiency.

photodarkening rate can be estimated using accelerated testing [(darkening of a short piece of fibre at a high ytterbium ion inversion level (near 50% and above)] and then modelling the operation of the ytterbium-doped fibre with allowance for the level of losses induced at a lower inversion level.

In our calculations, we used a power law relation between the photodarkening rate and ytterbium ion inversion, with an exponent of 6 [17]. We had to resort to this method for evaluating the darkening rate because direct photodarkening tests require a long time: from a few weeks to a year, depending on the darkening resistance of the fibre. Throughout this time, the specimen has to be exposed to the highest pump power. An accelerated test, which takes from a few tens of minutes to several hours, makes it possible to determine the coefficients in a relation describing the level of photoinduced losses (photodarkening) as a function of time and inverted population. In our case, we used a relation in the form of a stretched exponential function [16]:

$$T(t) = A\exp\left[-\left(\frac{t}{\tau}\right)^{\beta}\right] + (1 - A),$$

where T is the transmittance of the sample; τ is the time constant; β is the dispersion parameter; and $1 - A$ is the transmission level of the fibre after loss saturation is reached due to photodarkening. The dispersion parameter β is independent of the inversion level, whereas the time constant depends on it:

$$\tau(n) = \tau_0 (N/N_0)^6,$$

where N is the inverted population and τ_0 is the time constant at the inverted population N_0.

From our experimental $T(t)$ data, we evaluated the parameters τ_0, β and A. Next, we calculated τ for low inversion (in the laser/amplifier). In an accelerated darkening test, N_0 was estimated from known cross sections for ytterbium transitions and was further verified from the luminescence level. In the case of a laser or amplifier, the inversion level can be calculated by numerical methods at each point along the length of the fibre [18]. Variations in inversion over the cross section of the fibre were left out of consideration in our calculations.

Figure 5a show a schematic of the experimental setup used to measure photodarkening characteristics in fibres in accelerated mode. Under cladding pumping at a power of 26 W ($\lambda = 915$ nm), the inversion level in fibres 0.5 to 10 cm in length reaches 90%, which allows measurements to be made in about 1 h. The fibre length was chosen as a function of Yb concentration so as to rule out lasing and a high amplified luminescence level, while maintaining acceptable accuracy in photoinduced loss measurements. Figure 5b shows the initial optical loss spectrum and the loss spectrum after photodarkening (loss saturation level). The following parameters were obtained for the fibre under consideration: $\tau_0 = 6.9$ min, $\beta = 0.71$ and $A = 730$ dB m^{-1} at a wavelength of 500 nm. The photoinduced loss was measured as a function of time at a wavelength of 500 nm, which is more convenient and more accurate than direct photoinduced loss measurements at operating wavelengths (915 and 1064 nm), because they fall in the absorption bands of Yb and direct measurements are not always possible. Next, knowing a typical photoinduced loss spectrum of a given type of fibre (Fig. 5b), we converted the loss at $\lambda = 500$ nm to that at the operating wavelengths 915 and 1064 nm. The

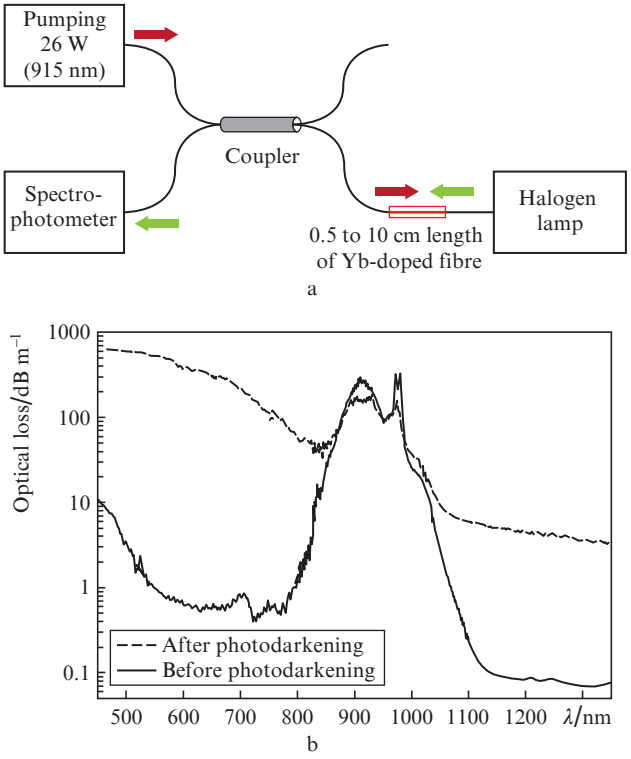

Figure 5. (a) Schematic of the system used to measure active fibre photodarkening in accelerated mode and (b) optical loss spectra of the ytterbium/fluorine codoped fibre before and after photodarkening.

resultant parameters were used to assess the output power degradation in an amplifier operating according to the scheme represented in Fig. 4a. Figure 6a shows the calculated output signal power as a function of time (counterpropagating pump power, 20 W; input signal power, 100 mW). In the case of the amplifier, the recalculated photodarkening rate turned out to be sufficiently low, and a marked drop in efficiency ($\sim$20%) should only be expected after 10 000 h of continuous laser operation. An active fibre with such characteristics fully satisfies relevant modern requirements.

For completeness, we fabricated a series of fibres similar in geometry and having identical aluminium and fluorine concentrations, but differing in ytterbium concentration. We measured the limiting level of 500-nm losses in the case of photodarkening for the entire series of the Yb-doped fibres, having both fluorine-free and fluorinated cores. Such experiments help to understand how fluorine influences the sensitivity of the fibres to photodarkening. Figure 6b presents the data obtained for the fluorine-free and fluorine-containing fibres at varied ytterbium concentration. In all of the fibres, the aluminium concentration was in the range 1.5–2.1 mol% and the germanium concentration was 0.3 to 0.5 mol%. The refractive index of the core in the fluorine-containing fibres ranged from 0.002 to 0.0025, and that in the fluorine-free fibres, from 0.006 to 0.007. It is seen in Fig. 6 that, at an average ytterbium content of $\sim$1.5 wt%, the limiting level of losses in the case of photodarkening in the fibres with a fluorine-doped core does not exceed the level of losses in conventional aluminosilicate fibres. At higher Yb concentrations, the loss even becomes slightly lower. This correlates with results reported by Schuster et al. [8], which demonstrate that fluorine helps to improve resistance to photodarkening. Thus, the proposed process for incorporating fluorine into ytterbium-doped aluminosilicate fibres allows the refractive index of their core to be substantially reduced (from 0.007 to 0–0.0025), without degrading their performance (lasing efficiency or resistance to photodarkening).

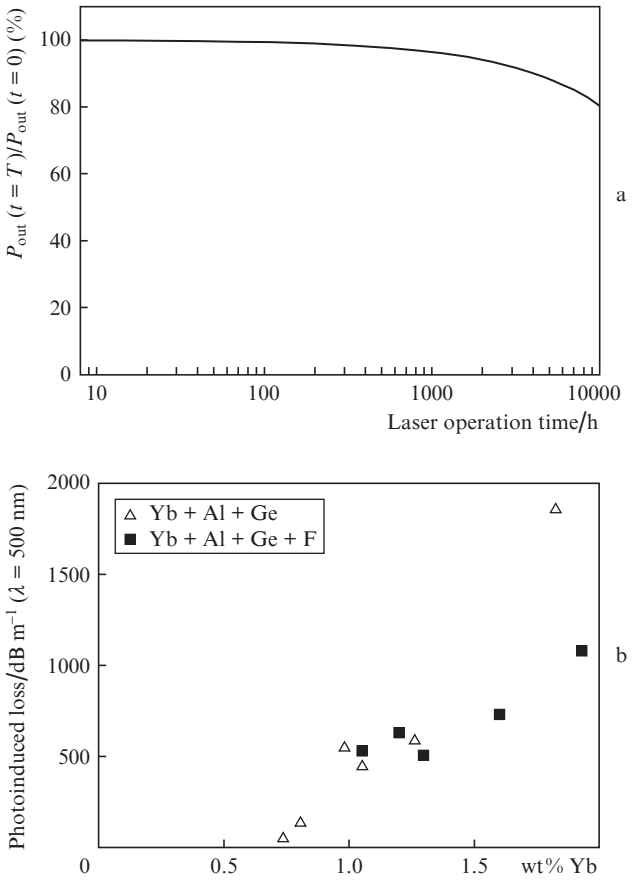

Figure 6. (a) Calculated output power of the amplifier as a function of time under photodarkening conditions and (b) influence of Yb concentration and fibre glass composition on the limiting level of photoinduced losses (photodarkening).

4. Conclusions

Aluminosilicate fibres with high fluorine concentrations (up to 2 wt%), high Yb^{3+} doping levels (up to 2 wt%) and a low refractive index of their core have been fabricated for the first time. We have studied their properties; measured their parameters, such as cladding pump absorption, lasing and amplification efficiency, and photodarkening parameters at a high inverted population and based on a model in which the photodarkening rate is a power law function of inverted population; and evaluated the degradation rate of the amplifier output power due to the photodarkening effect at a low population inversion level. The proposed fibre design has been shown to be very promising: it ensures a high cladding pump absorption rate (approximately twice that in commercially available optical fibres of similar geometry) and low photodarkening level (the laser output power was observed to drop by 20% only after 10 000 h of operation). We have compared the photodarkening resistance of the Yb-doped fibres with fluorinated and fluorine-free cores at various ytterbium concentrations.

The present results demonstrate that the proposed process allows one to incorporate high fluorine concentrations into ytterbium-doped aluminosilicate fibres without degrading their performance (lasing efficiency or resistance to photodarkening). The associated reduction in the refractive index of the fibre core allows one to produce fibres with a considerably increased core diameter, which is of importance from the viewpoint of the ability to raise the threshold for nonlinear effects.

Acknowledgements. This study was supported by the Russian Science Foundation (Grant No. 17-13-01343).

References

1. Arai K., Namikawa H., Kumata K., Honda T., Ishii Y., Handa T. *J. Appl. Phys.*, **59** (10), 3430 (1986).
2. Likhachev M.E., Bubnov M.M., Zotov K.V., Lipatov D.S., Yashkov M.V., Guryanov A.N. *Opt. Lett.*, **34**, 3355 (2009).
3. Likhachev M., Aleshkina S., Shubin A., Bubnov M., Dianov E., Lipatov D., Guryanov A. *Proc. CLEO/Europe-IQEC 2011* (Munich, Germany, 2011) paper CJ.P.24.
4. Kirchhof J., Unger S., Schwuchow A., Jetschke S., Knappe B. *Proc. SPIE*, **5723**, 261 (2005).
5. Kirchhof J., Unger S. *Proc. OFC Conf. 1999* (San Diego, CA, USA, 1999) paper WM1.
6. Guryanov A.N., Salganskii M.Yu., Khopin V.F., Kosolapov A.F., Semenov S.L. *Neorg. Mater.*, **45** (7), 887 (2009).
7. Mel'kumov M.A., Bufetov I.A., Kravtsov K.S., Shubin A.V., Dianov E.M. *Quantum Electron.*, **34**, 843 (2004) [*Kvantovaya Elektron.*, **34**, 843 (2004)].
8. Schuster K., Grimm S., Kalide A., Dellith J., Leich M., Schwuchow M., Langner A., Schötz G., Bartelt H. *Opt. Mater. Express*, **5** (4), 887 (2015).

9. Xu W., Yu C., Wang S., Lou F., Feng S., Wang M., Zhou Q., Chen D., Hu L., Guzik M. *Opt. Mater.*, **42**, 245 (2015).
10. Ballato J., Petit V., Tumminelli R.P., Minelly J.D., Khitrov V. *Proc. SPIE*, **9728**, 97282R (2016).
11. Wenbin Xu, Zhiquan Lin, Meng Wang, Suya Feng, Lei Zhang, Qinling Zhou, Danping Chen, Liyan Zhang, Shikai Wang, Chunlei Yu, Lili Hu. *Opt. Lett.*, **41**, 504 (2016).
12. Takahashi H., Oyobene A., Kosuge M. *Proc. 11th ECOC' 86* (Barcelona, 1986) pp 3–6.
13. Aksenov V.A., Ivanov G.A., Isaev V.A., Likhachev M.E. *Neorg. Mater.*, **46**, 1106 (2010).
14. Nagel S.R., MacChesney J.B., Walker K.L. *IEEE J. Quantum Electron.*, **18**, 459 (1982).
15. Mel'kumov M.A., Bufetov I.A., Bubnov M.M., Shubin A.V., Semenov S.L., Dianov E.M. *Quantum Electron.*, **35** (11), 996 (2005) [*Kvantovaya Elektron.*, **35** (11), 996 (2005)].
16. Koponen J., Soderlund M., Tammela S., Po H. *Proc. SPIE*, **5990**, 599008 (2005).
17. Shubin A.V., Yashkov M.V., Melkumov M.A., Smirnov S.A., Bufetov I.A., Dianov E.M. *Proc. CLEO/Europe-IQEC 2007* (Munich, Germany, 2007) paper CJ3–1.
18. Kelson Ido, Hardy Amos A. *IEEE J. Quantum Electron.*, **34** (9), 1570 (1998).